2025; 1-2 | 01-14

International Journal of Advances in Engineering and Computer Science
Volume 1, Issue 2, October-December 2025
(An Academians Publishers of Research & Academic Resources)

ISSN: 3121-6382

Original Research Article

Received: 28-09-2025 **Accepted**: 30-10-2025 **Published**: 05-11-2025

A Bivariate Chebyshev Integral Collocation Method for Solving One-Dimensional Heat Equation with Initial and Dirichlet Boundary Conditions

U.L.M. Althaf* **and M.A.A.M. Faham**
Department of Mathematical Sciences, Faculty of Applied Sciences, South Eastern University of Sri Lanka

Abstract: Partial differential equations (PDEs) play a vital role in modeling diverse physical and engineering processes, such as heat conduction and diffusion. However, obtaining analytical solutions is often difficult or impossible, which motivates the development of efficient numerical techniques. This paper presents a novel bivariate Chebyshev integral collocation method (BCICM) for solving the one-dimensional heat equation on the domain $[0,1] \times [0,1]$ with initial and Dirichlet boundary conditions. In the proposed method, the second-order spatial derivative in the governing PDE is approximated using a truncated bivariate shifted Chebyshev series of the first kind. By performing twofold integration, the approximate solution is reassembled while arbitrary integration functions are determined through boundary conditions. The time derivative is then evaluated analytically and substituted back into the heat equation, yielding an algebraic system for the unknown Chebyshev coefficients. Chebyshev-Gauss (CG) nodes in space and Chebyshev–Gauss–Lobatto (CGL) nodes in time are selected as collocation points to ensure the initial condition is imposed at $t = 0$. The entire procedure is implemented using MATLAB to efficiently compute the Chebyshev coefficients and approximate solutions. Three Numerical examples are presented to demonstrate the efficiency, rapid convergence, and accuracy of the proposed method.

Keywords: *Bivariate Chebyshev polynomials; Heat equation; Integral collocation; Chebyshev–Gauss–Lobatto nodes;*

1.0 Introduction

Partial differential equations (PDEs) are powerful mathematical tools used to model a wide range of dynamical systems in science, engineering, physics, biology, and economics. Solving a PDE involves determining an unknown function that satisfies the governing equation along with prescribed initial and/or boundary conditions.

Classical analytical techniques provide exact solutions for some special classes of PDEs; however, they are often restricted to simple geometries, constant coefficients, and specific boundary conditions. In many practical problems, obtaining analytical solutions is not feasible. To address these limitations, a variety of numerical approximation techniques have been developed to produce approximate solutions with error control.

Among various numerical approaches, polynomial approximation methods are particularly appealing due to their smoothness, continuous differentiability, and ease of implementation with modern computational tools. By the Weierstrass Approximation Theorem, any continuous real-valued function defined on a closed interval can be approximated arbitrarily well by a polynomial.

Several families of orthogonal polynomials have been employed for numerical

***Corresponding Author: U.L.M. Althaf (mohammedalf@gmail.com)**

approximation, including Taylor, Legendre, Gegenbauer, Hermite, and Chebyshev polynomials. Among them, Chebyshev polynomials are especially advantageous due to their *minimax* property, which minimizes the maximum approximation error. This makes them particularly effective for developing stable and highly accurate numerical schemes for differential equations.

Over the past decades, polynomial-based methods have been extensively applied to ordinary differential equations (ODEs) due to their accuracy and computational efficiency. Clenshaw (1957) introduced a Chebyshev series approach for linear differential equations, providing a systematic technique to compute the coefficients in the series. Later, Sezer and Kaynak (1996) developed the Chebyshev–matrix method, offering a matrix-based approach to obtain approximate polynomial solutions of linear differential equations. Akyüz and Sezer (2003) extended these ideas to systems of higher-order ODEs with variable coefficients, demonstrating the applicability of Chebyshev methods to more complex systems. These studies confirm that Chebyshev-based methods are well-established, accurate, and computationally efficient for a wide range of ODEs.

The application of Chebyshev techniques to partial differential equations (PDEs) has been comparatively less explored, particularly for multidimensional and nonlinear problems. Gumgum, Kurul, and Baykus Savasaneril (2018) applied Chebyshev collocation to the two-dimensional heat equation, while Karunakar and Chakraverty (2019) demonstrated the effectiveness of shifted Chebyshev polynomials PDEs. Lui and Nataj (2020) introduced a space–time Chebyshev spectral collocation scheme, improving accuracy in both spatial and temporal domains. More recently, Ghimire, Tian, and Lamichhane (2016), Lovetskiy, Sergeev, Kulyabov, and Sevastianov (2024), and Shior et al. (2024) applied Chebyshev-based methods to linear and nonlinear PDEs in engineering contexts. Despite these advances, the use of Chebyshev collocation for PDEs with diverse boundary and initial conditions remains less explored.

Motivated by this gap, the present work aims to develop an efficient Bivariate Chebyshev Integral Collocation Method (BCICM) that extends the conventional univariate framework to a bivariate integral collocation approach. The method provides a semi-analytical approximate solution for the one-dimensional heat equation with Dirichlet boundary and initial conditions.

2.0 Notations and Theory

2.1 Bivariate Chebyshev Polynomials

The univariate Chebyshev polynomial of the first kind of degree n, denoted by $T_n(x)$, is defined on the interval $[-1, 1]$ as:

$$T_n(x) = \cos(n\theta), \quad x = \cos\theta, \quad 0 \le \theta \le \pi, \quad n = 0, 1, 2, \ldots.$$

The corresponding bivariate Chebyshev polynomial of the same kind of degrees m and n over the domain $[-1, 1] \times [-1, 1]$ is defined as the product of two univariate Chebyshev polynomials:

$$T_{mn}(x, y) = T_m(x)T_n(y), \quad m, n = 0, 1, 2, \ldots.$$

2.2 Recurrence Relation

The univariate Chebyshev polynomials satisfy the recurrence relation

$$T_{n+1}(x) = 2xT_n(x) - T_{n-1}(x), \qquad n \ge 1,$$

with initial conditions $T_0(x) = 1$ and $T_1(x) = x$.

Similarly, the bivariate Chebyshev polynomials satisfy:

$$T_{(m+1)n}(x, y) = 2xT_{mn}(x, y) - T_{(m-1)n}(x, y),$$

$$T_{m(n+1)}(x, y) = 2yT_{mn}(x, y) - T_{m(n-1)}(x, y).$$

2. 3 Nodes of Chebyshev Polynomials

The nodes of Chebyshev polynomials, often referred to as zeros of Chebyshev polynomials, are widely used as collocation points in polynomial interpolation due to their excellent numerical properties.

The univariate Chebyshev polynomial $T_n(x)$, for $n \geq 1$ has n simple, real zeros within the interval $(-1, 1)$ and they are given by

$$x_j = \cos\left(\frac{2j+1}{2n}\pi\right), \qquad j = 0,1, \dots, (n-1).$$

This set of points is also known as the Chebyshev-Gauss (CG) nodes. A key characteristic of these nodes is that they are strictly interior points; the endpoints of the domain ($x = \pm 1$) are never included. Consequently, while ideal for many interpolations, CG nodes are less suitable for problems requiring the direct enforcement of boundary conditions at the endpoints of domain.

For problems where conditions must be imposed at the boundaries, the Chebyshev-Gauss-Lobatto (CGL) nodes are the preferred choice. These points are defined as the extrema of $T_n(x)$ on $[-1, 1]$and are given by:

$$x_j = \cos\left(\frac{j\pi}{n}\right), \qquad j = 0, 1, \cdots, n.$$

Unlike the CG nodes, the CGL set explicitly includes the endpoints ($j = 0 \Rightarrow x = 1,\ j = n \Rightarrow x = -1$) making it a natural grid for collocation methods in boundary value problems.

The bivariate CG nodes of $T_{mn}(x, y)$ are obtained as the tensor product of these univariate nodes in x- and y- directions:

$$(x_i, y_j) = \left(\cos\frac{2i+1}{2m}\pi\,, \cos\frac{2j+1}{2n}\pi\right),$$

$$i = 0,1, \dots, (m-1), \qquad j = 0,1, \dots, (n-1).$$

2.4 Chebyshev Polynomials on Generic Domain and Shifted Chebyshev Polynomials

The natural domain of the univariate Chebyshev polynomials is $[-1, 1]$. However, they can be mapped to any interval $[a, b]$ using the linear transformation:

$$\bar{x} = \frac{x - \frac{1}{2}(a+b)}{\frac{1}{2}(b-a)}.$$

In particular, when the interval is $[0, 1]$, the resulting polynomials are known as shifted Chebyshev Polynomials, denoted by $T_n^*(x)$ and are defined as

$$T_n^*(x) = T_n(2x - 1).$$

This concept extends naturally to the bivariate case. Mapping from $[-1, 1] \times [-1, 1]$ to a general domain $[a, b] \times [c, d]$ is achieved via

$$\bar{x} = \frac{x - \frac{1}{2}(a+b)}{\frac{1}{2}(b-a)}, \qquad \bar{y} = \frac{y - \frac{1}{2}(c+d)}{\frac{1}{2}(c-d)}.$$

The shifted bivariate Chebyshev polynomials are then defined as:

$$T_{mn}^*(x, y) = T_m^*(x) T_n^*(y),$$

$$m, n = 0, 1, 2, \dots.$$

2.5 Approximation of Functions Using Bivariate Chebyshev Polynomials

Any sufficiently smooth function $f(x, y)$ defined on a rectangular domain $[-1, 1] \times [-1, 1]$ can be approximated using a truncated bivariate Chebyshev series:

$$f(x, y) \approx \sum_{m=0}^{M}\sum_{n=0}^{N} a_{mn} T_{mn}(x, y)$$

$$= \sum_{m=0}^{M}\sum_{n=0}^{N} a_{mn} T_m(x) T_n(t),$$

where a_{mn} are the Chebyshev coefficients to be determined.

Using the orthogonality property of the Chebyshev polynomials with respect to the weight function $w(x,y) = \frac{1}{\sqrt{1-x^2}\sqrt{1-y^2}}$, the coefficients can be computed via continuous orthogonal projection**:**

$$a_{mn} = \frac{\alpha_m \alpha_n}{\pi^2} \int_{-1}^{1} \int_{-1}^{1} \frac{T_{mn}(x,y) f(x,y)}{\sqrt{1-x^2}\sqrt{1-y^2}} dxdy,$$

where the scaling factors are defined as

$$\alpha_k = \begin{cases} 1, & k = 0, \\ 2, & k \geq 1. \end{cases}$$

In practice, the integrals are often approximated using discrete orthogonal projection at the CG nodes as follows:

$$a_{mn} \approx \frac{\alpha_m \alpha_n}{MN} \sum_{i=0}^{M-1} \sum_{j=0}^{N-1} f(x_i, y_j) T_{mn}(x_i, y_j),$$

where (x_i, x_j), $i = 0,1,\dots,(M-1)$, $j = 0,1,\dots,(N-1)$, are bivariate CG nodes, and α_k is defined as above.

3.0 Methodology

(i). Problem Definition

We consider the one-dimensional heat conduction equation

$$u_t = \alpha u_{xx}, \qquad 0 < x < 1, \qquad t > 0,$$

subject to the initial and Dirichlet boundary conditions

$$u(x,0) = u_0(x), \qquad u(0,t) = \gamma_0(t), \qquad u(1,t) = \gamma_1(t), \tag{1}$$

where $\alpha > 0$ is the thermal diffusivity constant.

(ii). Approximation of u_{xx} using Bivariate Shifted Chebyshev Expansion

The second-order spatial derivative $u_{xx}(x,t)$ is approximated by a finite double series expansion in shifted bivariate Chebyshev polynomials over

$$u_{xx}(x,t) \approx \sum_{m=0}^{M} \sum_{n=0}^{N} a_{mn} T^*_{mn}(x,t) = \sum_{m=0}^{M} \sum_{n=0}^{N} a_{mn} T^*_m(x) T^*_n(t), \tag{2}$$

where a_{mn} are unknown coefficients to be determined and $T^*_k(x)$ denotes the shifted Chebyshev polynomial of degree k defined on the interval $[0,1]$.

(iii). Integration with Respect to x

Integrating equation (2) twice with respect to x gives an approximation for $u(x,t)$:

$$u(x,t) \approx \sum_{m=0}^{M} \sum_{n=0}^{N} a_{mn} \overline{T^*_m}(x) T^*_n(t) + x g(t) + h(t), \tag{3}$$

where $\overline{T^*_m}(x)$ denotes the twice-integrated form of $T^*_m(x)$, and $g(t)$, $h(t)$ are arbitrary functions of t arising from integration constants.

(iv). Enforcement of Dirichlet Boundary Conditions

Applying the boundary conditions $u(0,t) = \gamma_0(t)$ and $u(1,t) = \gamma_1(t)$ to equation (3):

Evaluate (3) at $x = 0$:

$$u(0,t) = \gamma_0(t) = \sum_{m=0}^{M}\sum_{n=0}^{N} a_{mn}\overline{T_m^*}(0)T_n^*(t) + h(t),$$

yielding

$$h(t) = \gamma_0(t) - \sum_{m=0}^{M}\sum_{n=0}^{N} a_{mn}\overline{T_m^*}(0)T_n^*(t). \quad (4)$$

Evaluate (3) at $x = 1$:

$$u(1,y) = \gamma_1(t) = \sum_{m=0}^{M}\sum_{n=0}^{N} a_{mn}\overline{T_m^*}(1)T_n^*(t) + g(t) + h(t).$$

$$\Longrightarrow g(t) = \gamma_1(t) - \sum_{m=0}^{M}\sum_{n=0}^{N} a_{mn}\overline{T_m^*}(1)T_n^*(t) - h(t).$$

Eliminating $h(t)$ using equation (4), we obtain

$$g(t) = \gamma_1(t) - \gamma_0(t) - \sum_{m=0}^{M}\sum_{n=0}^{N} a_{mn}\left(\overline{T_m^*}(1) - \overline{T_m^*}(0)\right)T_n^*(t). \quad (5)$$

Now substituting $g(t)$ and $h(t)$ using equations (4) and (5) gives

$$u(x,t) \approx \sum_{m=0}^{M}\sum_{n=0}^{N} a_{mn}\Psi_m(x)T_n^*(t) + x\gamma_1(t) + (1-x)\gamma_0(t), \quad (6)$$

where

$$\Psi_m(x) = [\overline{T_m^*}(x) - x\overline{T_m^*}(1) - (1-x)\overline{T_m^*}(0)].$$

(v). Computation of u_t

Differentiating equation (6) partially with respect to t, we obtain:

$$u_t(x,t) = \sum_{m=0}^{M}\sum_{n=0}^{N} a_{mn}\Psi_m(x)T_n^{*\prime}(t) + x\gamma_1{}'(t) + (1-x)\gamma_0{}'(t)\,. \quad (7)$$

(vi). Substitution into the Heat Equation

Substituting equations (2) and (7) into the governing PDE (1) gives:

$$\sum_{m=0}^{M}\sum_{n=0}^{N} a_{mn}[\Psi_m(x)T_n^{*\prime}(t) - \alpha T_m^*(x)T_n^*(t)] = (x-1)\gamma_0{}'(t) - x\gamma_1{}'(t). \quad \mathbf{(8)}$$

(vii). Collocation Strategy

From equation (6), there are a total of $(M+1)(N+1)$ unknown coefficients a_{mn} to be determined in order to construct the approximate solution $u(x,t)$. However, it is important to note that the initial condition has not yet been incorporated into the formulation. To address this, appropriate collocation strategy is introduced as follows.

Since the boundary conditions have already been employed to eliminate the arbitrary functions $g(t)$ and $h(t)$ arising from the twofold integration of the double Chebyshev expansion of u_{xx}, it is desirable to use pure shifted CG nodes of T^*_{M+1} as collocation points for spatial variable *x*. These nodes are defined by

$$x_i^* = \frac{1}{2}\left(1+\cos\left(\frac{(2i+1)}{2(M+1)}\right)\pi\right),$$

$$i = 0, 1, \cdots, M.$$

These $(M+1)$ nodes lie strictly within the open interval $(0,1)$, thereby excluding the endpoints $x=0$ and $x=1$ that are already accounted for through the imposed boundary conditions. This choice effectively avoids redundancy in the system of equations.

To incorporate the initial condition into the collocation framework, the shifted Chebyshev–Gauss–Lobatto (CGL) nodes are adopted for the temporal variable t, given by

$$t_j^* = \frac{T}{2}\left(1-\cos\left(\frac{j\pi}{N}\right)\right), \quad j = 0, 1, \cdots, N,$$

Where T denotes the upper bound of the temporal domain. For simplicity, we set $T=1$, allowing the direct use of shifted CGL nodes within the interval $[0,1]$. These $(N+1)$ nodes include both endpoints of the interval, ensuring that $t=0$ (corresponding to $j=0$) is explicitly present. Hence, the initial condition is naturally incorporated into the collocation process, while maintaining high accuracy near the boundaries due to the clustering property of the CGL nodes.

The collocation points $(x_i^*,\ t_0^*=0)$ for $i=0,1,\cdots,M$ are substituted into equation (6) to incorporate the initial condition. This yields $(M+1)$ equations involving the unknown coefficients a_{mn} $(i=0,1,\cdots,M;\ j=1,2,\cdots,N)$ as follows:

$$\sum_{m=0}^{M}\sum_{n=0}^{N} a_{mn}\Psi_m(x_i^*)T_n^*(0) = u_0(x_i^*) - x_i^*\gamma_1(0) - (1-x_i^*)\gamma_0(0). \tag{9}$$

Similarly, the collocation points $(x_i^*,\ t_k^*)$ for $i=0,1,\cdots,M$ and $j=1,2,\cdots,N$ are applied to equation (8) to enforce the governing partial differential equation.

This results in $N(M+1)$ additional equations for the remaining unknown coefficients a_{mn} $(i=0,1,\cdots,M;\ j=1,2,\cdots,N)$:

$$\sum_{m=0}^{M}\sum_{n=0}^{N} a_{mn}\left[\Psi_m(x_i^*)T_n^{*'}(t_j^*) - \alpha T_m^*(x_i^*)T_n^*(t_j^*)\right] = -x_i^*\gamma_1{}'(t_j^*) - (1-x_i^*)\gamma_0{}'(t_j^*). \tag{10}$$

Combining equations (9) and (10), we obtain a total of $(M+1)(N+1)$ linear algebraic equations for the $(M+1)(N+1)$ unknown coefficients a_{mn}. This system can be written compactly in matrix form as:

Available Online: https://academianspublishers.org/international-journal-of-advances-in-engineering-and-computer-science/

$$\left[\varphi_{mn}^{ij}\right]_{P\times P} \times [a_{mn}]_{P\times 1} = \left[b^{ij}\right]_{P\times 1}, \tag{11}$$

where $P = (M+1)(N+1)$, a_{mn} are unknown coefficients to be determined and the matrix entries are defined as:

$$\varphi_{mn}^{ij} = \begin{cases} \Psi_m(x_i^*)T_n^*(0), & i = 0,1,\cdots,M;\ j = 0, \\ \Psi_m(x_i^*)T_n^{*\prime}(t_j^*) - \alpha T_m^*(x_i^*)T_n^*(t_j^*), & i = 0,1,\cdots,M;\ j = 1,2,\cdots,N, \end{cases}$$

and

$$b^{ij} = \begin{cases} u_0(x_i^*) - x_i^*\gamma_1(0) - (1-x_i^*)\gamma_0(0), & i = 0,1,\cdots,M;\ j = 0, \\ -x_i^*\gamma_1{}'(t_j^*) - (1-x_i^*)\gamma_0{}'(t_j^*), & i = 0,1,\cdots,M;\ j = 1,2,\cdots,N. \end{cases}$$

Solving the linear system (11) provides all unknown coefficients a_{mn}, which are then substituted back into equation (6) to reconstruct the approximate solution u_approx over the spatial–temporal domain.

Since our procedure begins by expanding the second derivative of the unknown function $u(x,t)$ with respect to the spatial variable x in terms of truncated bivariate Chebyshev polynomials up to degree M and N in x and t, respectively, and the unknown function is subsequently recovered through a two-fold integration, the resulting approximate polynomial solution attains a maximum degree of $(M+2)$ in x, while the temporal variable t remains bounded by a maximum degree of N.

4.0 Results and Discussion

To validate the effectiveness of the proposed BCICM, three one-dimensional heat conduction equations are investigated. These examples include cases with homogeneous and non-homogeneous Dirichlet boundary conditions and involve both polynomial and non-polynomial exact solutions. The numerical approximations are compared against analytical solutions, and convergence behavior is analyzed in terms of the spatial and temporal polynomial degrees M and N.

Example 1: Homogeneous Boundary Conditions with an Infinite Series Exact Solution

We consider

$$u_t = u_{xx}, \qquad 0 < x < 1, \qquad t > 0,$$

subject to homogeneous Dirichlet boundary conditions

$$u(0,t) = 0, \qquad u(1,t) = 0, \qquad t > 0,$$

and the initial temperature distribution

$$u(x,0) = x(1-x), \qquad 0 < x < 1.$$

The exact analytical solution is represented by the Fourier sine series:

$$u(x,t) = \sum_{n=1}^{\infty} \frac{4}{n^3\pi^3}[1-(-1)^n]\sin(n\pi x)e^{-n^2\pi^2 t}.$$

Using the proposed BCICM, the MATLAB-generated approximate solution u_approx for Example 1 with $M = 2$ and $N = 2$ is obtained as follows:

```
u_approx = -0.41591*t^2*x^4 +
0.83183*t^2*x^3 - 1.994*t^2*x^2 +
1.5781*t^2*x + 0.38251*t*x^4 -
0.76503*t*x^3 + 2.9975*t*x^2 -
2.615*t*x -2.3709e-16*x^4 + 3.367e-
16*x^3 - 1.0*x^2 + 1.0*x
```

It is evident from this polynomial representation that the highest degree in x is 4 (i.e., $M + 2$) and the highest degree in t is 2 (i.e., N). This observation is in perfect agreement with the theoretical expectation:

Since the exact solution is expressed as an infinite series, we truncate the series at $n = 30$ and treat this truncated form as the exact solution for the purpose of comparison with the approximate solution.

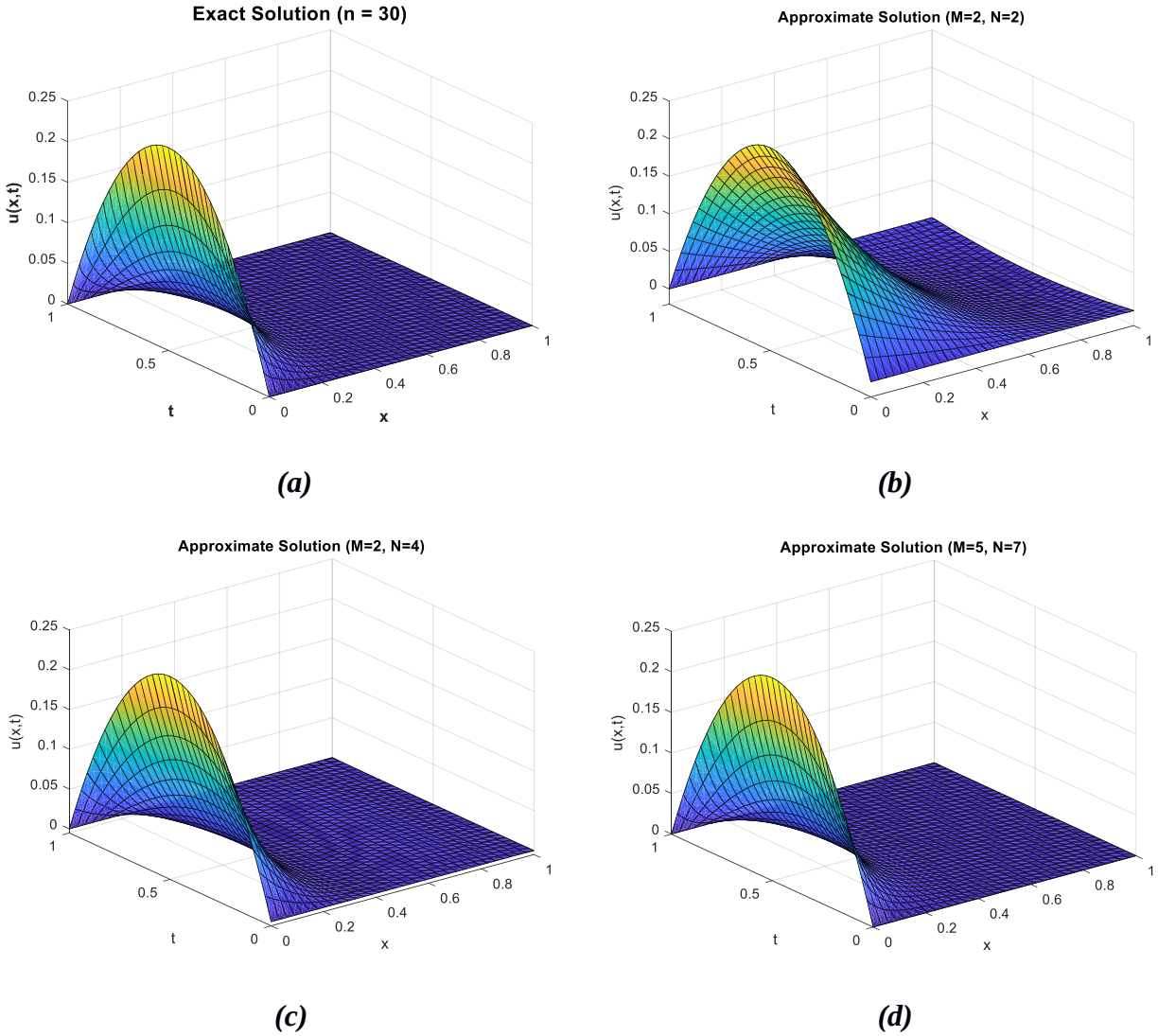

Figure 01: *(a) Exact analytical solution and (b)–(d) BCICM approximate solutions with increasing polynomial degrees (M, N) for Example 1.*

Above, Figure 01(a) displays the exact analytical solution of Example 1, while Figures 01(b)–(d) present the numerical approximations obtained using the proposed BCICM for different combinations of polynomial degrees (M, N). As the values of M and N increase, the approximate solutions exhibit noticeable improvements in spatial–temporal accuracy and closely follow the behavior of the exact solution. These visual results clearly demonstrate the convergence characteristics of the proposed method.

M, N	Maximum Absolute Error
M=2, N=2	*9.89906e-02*
M=1, N=3	*2.32573e-02*
M=2, N=4	*8.96684e-03*
M=4, N=6	*1.65589e-03*
M=5, N=7	*3.03599e-04*
M=7, N=5	*2.39561e-03*
M=5, N=8	*4.76440e-04*
M=8, N=10	*1.65164e-04*

Table 01: *Maximum absolute error for Example 1 under different* (M, N) *combinations, evaluated on a uniform spatial–temporal grid with a step size of* 0.2.

Table 01 presents the maximum absolute errors computed on a uniform spatial-temporal grid with step size 0.2 for various polynomial degree combinations (M, N). The results demonstrate a systematic reduction in error as the polynomial degrees increase, with the maximum error decreasing from 9.89906×10^{-2} for $(M, N) = (2, 2)$ to 1.65164×10^{-4} for $(M, N) = (8, 10)$. This consistent error reduction confirms the spectral convergence properties of the proposed BCICM. The observed non-monotonic behavior in select cases, particularly the comparison between $(M = 7,\ N = 5)$ with error 2.39561×10^{-3} and $(M = 5,\ N = 7)$ with error 3.03599×10^{-4} reveals an important interplay between spatial and temporal resolution requirements, suggesting that optimal accuracy depends on balanced refinement in both dimensions rather than maximizing either parameter independently.

	$x = 0.0$	$x = 0.2$	$x = 0.4$	$x = 0.6$	$x = 0.8$	$x = 1.0$
$t = 0.0$	*0.00000e+00*	*1.00820e-06*	*6.26720e-07*	*6.26720e-07*	*1.00820e-06*	*3.92010e-17*
$t = 0.2$	*0.00000e+00*	*1.65160e-04*	*9.46420e-05*	*9.46420e-05*	*1.65160e-04*	*4.38920e-18*
$t = 0.4$	*0.00000e+00*	*1.59480e-04*	*1.09840e-04*	*1.09840e-04*	*1.59480e-04*	*6.09710e-19*
$t = 0.6$	*0.00000e+00*	*1.39760e-04*	*9.04460e-05*	*9.04460e-05*	*1.39760e-04*	*8.46960e-20*
$t = 0.8$	*0.00000e+00*	*1.55560e-05*	*6.54210e-06*	*6.54210e-06*	*1.55560e-05*	*1.17650e-20*
$t = 1.0$	*0.00000e+00*	*7.36630e-06*	*4.93290e-06*	*4.93280e-06*	*7.36640e-06*	*1.63430e-21*

Table 02: *Point wise absolute error distribution for Example 1 corresponding to* $(M, N) = (8,10)$, *evaluated on a uniform spatial grid with step size* 0.2 *and time step* 0.2.

Table 02 provides the point wise error distribution on the same uniform grid of step size 0.2 for the case $(M, N) = (8,10)$. Due to the exact enforcement of Dirichlet boundary conditions, the numerical error at the boundaries remains nearly zero. Across the interior nodes, the error remains extremely small at all-time levels, demonstrating the reliability and robustness of the method throughout the computational domain.

Example 2: Non-Homogeneous Boundary Conditions with Finite-Term Exact Solution

We next consider the following one-dimensional heat equation:

$$u_t = 3u_{xx}, \qquad 0 < x < 1, \qquad t > 0,$$

subject to the boundary conditions

$$u(0, t) = 0, \qquad u(1, t) = 1, \qquad t > 0,$$

and the initial condition

$$u(x, 0) = x + \sin(\pi x), \qquad 0 < x < 1.$$

The exact solution of the above PDE is

$$u(x, t) = x + e^{-3\pi^2 t} \sin(\pi x).$$

The MATLAB generated approximate solution *u_approx* for Example 2; computed via the proposed BCICM with $M = 1, N = 3$, expressed as:

```
u_approx = -3.2052e-15*t^3*x^3 +
16.596*t^3*x^2 - 16.596*t^3*x +
6.4772e-15*t^2*x^3 - 34.23*t^2*x^2 +
34.23*t^2*x - 3.8962e-15*t*x^3 +
21.134*t*x^2 - 21.134*t*x + 6.2804e-
16*x^3 - 3.5521*x^2 + 4.5521*x
```

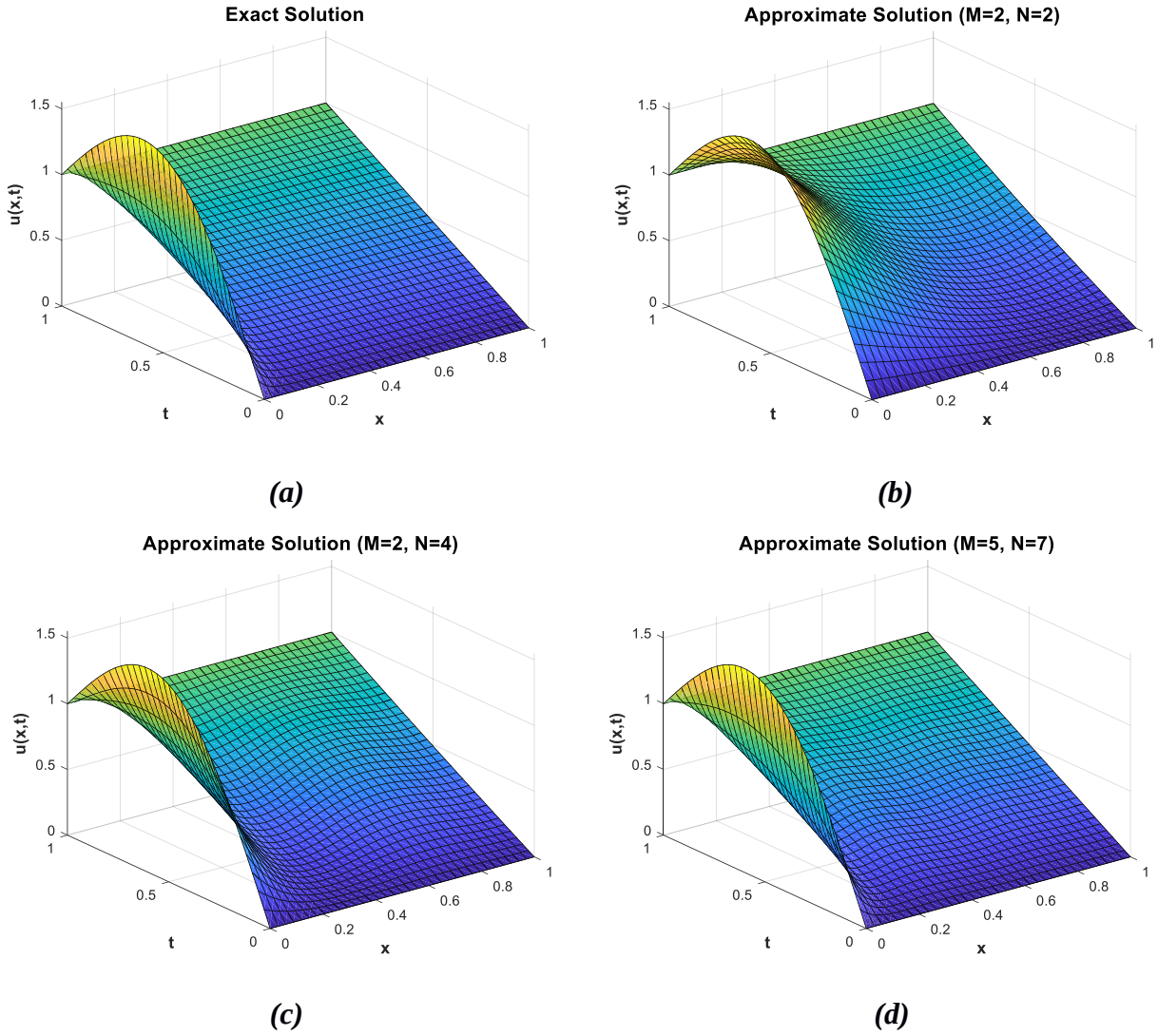

Figure 02: *(a) Exact analytical solution and (b)–(d) BCICM approximate solutions with increasing polynomial degrees (M, N) for Example 2.*

Figure 02 (b)–(d) shows that the approximate solutions for Example 2 increasingly resemble the exact solution depicted in Figure 02(a) as the polynomial degrees are increased.

M, N	**Maximum Absolute Error**
M=2, *N*=2	*4.78743e-01*
M=1, *N*=3	*1.32250e-01*
M=2, *N*=4	*9.12547e-02*
M=4, *N*=6	*5.97661e-02*
M=5, *N*=7	*1.41425e-02*
M=7, *N*=5	*8.80991e-02*
M=5, *N*=8	*1.15563e-02*
M=8, *N*=10	*4.68940e-03*
M=12, *N*=14	*1.18728e-04*

Table 03: *Maximum absolute error for Example 2 under different (M, N) combinations, evaluated on a uniform spatial–temporal grid with a step size of 0.2.*

Table 03 reports the maximum absolute errors for Example 2 obtained using different combinations of (M, N). As expected, the error decreases progressively when the polynomial degrees in both the spatial and temporal domains are increased, confirming the convergence of the proposed BCICM.

However, the reduction rate is slightly lower compared to Example 1, which may be attributed to the inhomogeneous nature of the boundary conditions in this problem.

Furthermore, a distinct deviation in error can be observed for the cases $(M, N) = (5, 7)$ and $(7, 5)$. Although both settings involve relatively high polynomial degrees, the resulting errors exhibit a noticeable difference. This behavior can be explained by the imbalance in spatial–temporal resolution under the BCICM formulation. Specifically, when $M = 7$ and $N = 5$, the effective spatial degree becomes 9, while the temporal degree remains 7, leading to a resolution mismatch that negatively affects the approximation accuracy. Conversely, $(M, N) = (5, 7)$ maintains a more balanced resolution between the spatial and temporal domains, yielding a lower error.

These findings highlight that selecting polynomial degrees that maintain a balanced approximation degree in both dimensions leads to better accuracy, further supporting the observations made in Example 1.

	$x = 0.0$	$x = 0.2$	$x = 0.4$	$x = 0.6$	$x = 0.8$	$x = 1.0$
$t = 0.0$	*0.00000e+00*	*4.88500e-15*	*1.11020e-15*	*8.88180e-16*	*5.32910e-15*	*1.55430e-15*
$t = 0.2$	*0.00000e+00*	*7.33780e-05*	*1.18730e-04*	*1.18730e-04*	*7.33780e-05*	*8.85960e-14*
$t = 0.4$	*0.00000e+00*	*4.97290e-05*	*8.04640e-05*	*8.04640e-05*	*4.97290e-05*	*6.43060e-12*
$t = 0.6$	*0.00000e+00*	*6.56370e-05*	*1.06200e-04*	*1.06200e-04*	*6.56370e-05*	*5.01890e-11*
$t = 0.8$	*0.00000e+00*	*4.02350e-05*	*6.51020e-05*	*6.51020e-05*	*4.02350e-05*	*4.11780e-10*
$t = 1.0$	*0.00000e+00*	*1.25890e-06*	*2.03700e-06*	*2.03710e-06*	*1.25920e-06*	*4.02660e-10*

Table 04: *Point wise absolute error distribution for Example 2 corresponding to* $(M, N) = (12,14)$, *evaluated on a uniform spatial grid with step size* 0.2 *and time step* 0.2.

Table 04 displays the point wise absolute error distribution for Example 2 using BCICM with polynomial degrees $(M, N) = (12,14)$ evaluated on a uniform spatial-temporal grid with step size 0.2. The results reveal exceptional boundary condition treatment, with errors at the spatial boundaries $x = 0$ and $x = 1$ maintaining near-machine precision levels (10^{-14} to 10^{-10}), confirming the exact enforcement of Dirichlet boundary conditions. Notably, the initial condition at $t = 0$ also achieves remarkable accuracy, with errors on the order of 10^{-15} to 10^{-16}, demonstrating precise satisfaction of the initial condition.

Example 3: Non-Homogeneous Dirichlet Boundary Conditions with Exact Polynomial Solution

Finally, consider:

$$u_t = 2u_{xx}, \qquad 0 < x < 1, \qquad t > 0,$$

subject to non-homogeneous Dirichlet boundary conditions

$$u(0, t) = 48t^2 + 12t - 1,$$

$$u(1, t) = 48t^2 + 12t + 1, \quad t > 0,$$

and the initial condition

$$u(x, 0) = x^4 - 2x^3 + 3x^2 - 1,$$
$$0 < x < 1.$$

The closed form polynomial solution is:

$$u(x,t) = x^4 - 2x^3 + 24x^2t + 3x^2 - 24tx + 48t^2 + 12t - 1.$$

For Example 3, the MATLAB computation with polynomial degrees $(M,N) = (2,2)$ yields the approximate solution:

```
u_approx = 1.1605e-14*t^2*x^4 -
3.1162e-14*t^2*x^3 + 2.5597e-
14*t^2*x^2 - 6.0409e-15*t^2*x +
48.0*t^2 - 1.7813e-14*t*x^4 +
4.7464e-14*t*x^3 + 24.0*t*x^2 -
24.0*t*x + 12.0*t + 1.0*x^4 -
2.0*x^3 + 3.0*x^2 - 1.4501e-15*x -
1.0
```

The terms corresponding to $48t^2 + 24tx^2 - 24tx + 12t + x^4 - 2x^3 + 3x^2 - 1$ exactly match the exact solution, while the remaining coefficients are of order $\boldsymbol{\mathcal{O}(10^{-14})}$, demonstrating that the proposed BCICM achieves near-machine precision accuracy.

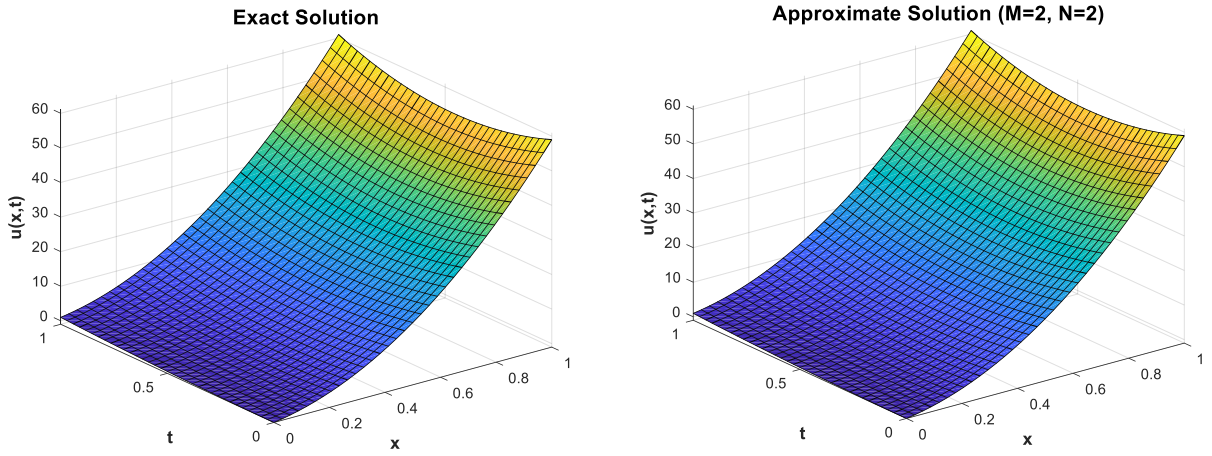

(a) ***(b)***

Figure 03: *(a) Exact analytical solution and (b) BCICM approximate solution with* $(M{=}2,N{=}2)$ *for Example 3.*

	$x = 0.0$	$x = 0.2$	$x = 0.4$	$x = 0.6$	$x = 0.8$	$x = 1.0$
$t = 0.0$	*0.00000e+00*	*0.00000e+00*	*2.22040e-16*	*6.66130e-16*	*8.88180e-16*	*8.88180e-16*
$t = 0.2$	*0.00000e+00*	*4.44090e-16*	*8.88180e-16*	*0.00000e+00*	*8.88180e-16*	*1.77640e-15*
$t = 0.4$	*0.00000e+00*	*1.77640e-15*	*1.77640e-15*	*0.00000e+00*	*3.55270e-15*	*1.77640e-15*
$t = 0.6$	*0.00000e+00*	*0.00000e+00*	*0.00000e+00*	*3.55270e-15*	*3.55270e-15*	*3.55270e-15*
$t = 0.8$	*0.00000e+00*	*7.10540e-15*	*0.00000e+00*	*7.10540e-15*	*7.10540e-15*	*0.00000e+00*
$t = 1.0$	*0.00000e+00*	*7.10540e-15*	*7.10540e-15*	*7.10540e-15*	*1.42110e-14*	*0.00000e+00*

Table 05: *Point wise absolute error distribution for Example 3 corresponding to* $(M,N) = (2,2)$*, evaluated on a uniform spatial grid with step size* 0.2 *and time step* 0.2.

Figure 03 (a) and (b) illustrate the comparison between the exact analytical solution and the approximate solution for Example 3 with polynomial degrees $(M,N) = (2,2)$. As shown, the BCICM solution closely follows the exact solution across the spatial and temporal domain. The point wise absolute error distribution, presented in Table 05, confirms that the discrepancies remain extremely

small, with values on the order of 10^{-15} throughout most of the domain. The maximum absolute error is 1.4211×10^{-14}, demonstrating that the proposed BCICM achieves near-machine precision and provides highly accurate approximation.

5.0 Conclusion

In this study, a novel bivariate Chebyshev integral collocation method (BCICM) was developed for solving the one-dimensional heat equation with Dirichlet boundary and initial conditions. The proposed approach leverages a truncated bivariate shifted Chebyshev series to approximate the spatial derivatives, reconstructing the solution through twofold integration while enforcing boundary conditions. By employing Chebyshev nodes in space and Chebyshev–Gauss–Lobatto (CGL) nodes in time, the method incorporates initial condition, resulting in a semi-analytical solution that is valid over the entire spatial-temporal domain rather than solely at discrete grid points, a key advantage over classical numerical methods.

The method was applied to three numerical examples, demonstrating rapid convergence, high accuracy, and excellent agreement with exact solutions. Notably, for cases where the exact solution is polynomial, the BCICM yields near-machine precision polynomial approximations.

6.0 Future Work

Rigorous analysis can be performed to optimally select the polynomial degrees (M, N) for a desired level of accuracy. Moreover, the BCICM can be extended to other types of partial differential equations, including wave, diffusion–reaction, and heat equations with source terms, under various boundary conditions such as Neumann or mixed conditions. Additionally, the method is extended to arbitrary spatial-temporal domains, further enhancing its flexibility and suitability for a wide range of complex physical and engineering problems.

Conflict of Interest

The authors declare that there is no conflict of interest regarding the publication of this paper.

References

Clenshaw, C. W. (1957). The numerical solution of linear differential equations in Chebyshev series. Mathematical Proceedings of the Cambridge Philosophical Society, 53(01), 134.

El-Gendi, S. E. (1975). On Chebyshev solution of parabolic partial differential equations. IMA Journal of Applied Mathematics, 16(3), 283–289. https://doi.org/10.1093/imamat/16.3.283.

M. Sezer and M. Kaynak, “Chebyshev Polynomial Solutions of Linear Differential Equations,” International Journal of Mathematical Education in Science & Technology, Vol. 27, No. 4, 1996, pp. 607-618. doi:10.1080/0020739960270414.

Akyüz, O. T., & Sezer, M. (2003). Chebyshev polynomial solutions of systems of high-order linear differential equations with variable coefficients. Applied Mathematics and Computation, 140(1), 49–60. doi.org/10.1016/S0096-3003(02)00403-4.

Avazzadeh, Z., & Heydari, M. H. (2012). Chebyshev polynomials for solving two-dimensional linear and nonlinear integral equations of the second kind. Computational & Applied Mathematics, 31(1), 127–142. https://doi.org/10.1590/S1807-03022012000100007 .

G. Y¨uksel, O.R. Is¸ık, M. Sezer, Error analysis of the Chebyshev collocation method for linear second-order partial differential equations, International Journal of Computer Mathematics, (2014), http://dx.doi.org/10.1080/00207160.2014.966099

Ghimire, B., Tian, H., Lamichhane, A. (2016). Numerical Solutions of Elliptic Partial Differential Equations using Chebyshev Polynomials. Computers and

Mathematics with Applications, 72(4), 1042-1054.

Mahdy, A. (2017). Second kind shifted Chebyshev polynomials for solving the model nonlinear ODEs. American Journal of Computational Mathematics, 7(4), 391–401. https://doi.org/10.4236/ajcm.2017.74028

Kumar, D., Upadhyay, S., Singh, S., & Rai, K. (2017). Legendre wavelet collocation solution for system of linear and nonlinear delay differential equations. International Journal of Applied and Computational Mathematics, 3, Article 356. https://doi.org/10.1007/s40819-017-0356-y

Gumgum, S., Kurul, E., & Baykus Savasaneril, N. (2018). Chebyshev collocation method for the two-dimensional heat equation. Communication in Mathematical Modeling and Applications, 3(2), 1–8.

Karunakar, P., & Chakraverty, S. (2019). Shifted Chebyshev polynomials based solution of partial differential equations. 1(4), 1–9. https://doi.org/10.1007/S42452-019-0292-Z.

Lui, S. H., & Nataj, S. (2020). Chebyshev spectral collocation in space and time for the heat equation. 52, 295–319. https://doi.org/10.1553/ETNA_VOL52S295.

Lovetskiy, K., Sergeev, S., Kulyabov, D., & Sevastianov, L. (2024). Application of the Chebyshev collocation method to solve boundary value problems of heat conduction. Discrete and Continuous Models and Applied Computational Science, 32(1), 74–85. https://doi.org/10.22363/2658-4670-2024-32-1-74-85

Shior, M. M., Agbata, B. C., Obeng–Denteh, W., Kwabi, P. A., Ezugorie, I. G., Marcos, S., Asante-Mensa, F., & Abah, E. (2024). Numerical solution of partial differential equations using MATLAB: Applications to one-dimensional heat and wave equations. Deleted Journal, 23(4), 243–254. https://doi.org/10.4314/sa.v23i4.21